ANALYSIS OF A COUNTERFLOW HEAT EXCHANGER WITH HELICAL CHANNELS ENABLED BY ADDITIVE MANUFACTURING

[1]Aravindakshan Thirumalai Ananthanpillai, [2]Jedediah Storey, [3]Daniel Kirk

[1]PhD Student,[2]PhD Student,[3]Professor
[1]Mechanical Engineering, [2,3]Aerospace Engineering
[1,2,3]Florida Institute of Technology, Melbourne,USA
[1]ta.aravindakshan@gmail.com, [2]jstorey2009@my.fit.edu, [3]dkirk@fit.edu

Abstract*—Compact heat exchangers are desirable in many aerospace applications. New additive manufacturing approaches, such as 3D printing, have enabled heat exchanger geometries that cannot be fabricated using conventional approaches. The new geometries enabled by 3D printing result in more efficient heat transfer using more compact devices. However, the 3D printing process also imposes fabrication constraints which lead to potential performance degradations such as greater frictional pressure loss of the working fluids. This paper presents the design and analysis of a novel counter flow heat exchanger which uses helically shaped fluid channels to enhance heat transfer. An analytical model is developed to trade the size and mass of the device versus required heat transfer performance and acceptable levels of fluid pressure loss.Counterflow heat exchangers with helically shaped fluid channels offer an improved heat transfer rate as compared with straight fluid channels A tradeoff between frictional pressure loss, mass, and volume compactness is used to optimize the design of an additively manufactured heat exchanger for in-space applications.

***IndexTerms*—Counterflow heat exchanger, Secondary flows, Heat transfer and volume compactness, Additive manufacturing, Parametric study.**

I. INTRODUCTION

Thermal management using heat exchangers are common in many aerospace applications and especially important for spacecraft. In addition to providing effective thermal control, there is strong motivation to increase the compactness by reducing the mass and volume of the heat exchanger device [1]. Rockets and spacecraft employ a wide array of different heat exchanger types [2-7].

New advances in additive manufacturing are further enabling the development of more highly compact, higher performance, and lighter weight heat exchangers which cannot be easily or cost-effectively manufactured using conventional approaches [8-12]. Direct Metal Laser Sintering (DMLS) allows for the direct manufacturing of complex parts and combines the design flexibility of 3D printing with the mechanical properties of the metal. Additively manufactured components, including heat exchangers, are becoming prevalent in spacecraft applications [13-15].

Although there are many new additively manufactured heat exchanger geometries under consideration, many of these concepts suffer from unacceptable performance degradations. For example, 3D printed heat exchangers that use complex internal flow passage geometries are highly compact, but the frictional pressure loss of the working fluid is often too high for rocket and spacecraft applications.

One of the most useful devices is the counterflow heat exchanger which can be designed to achieve high heat transfer effectiveness and offers acceptable levels of working fluid pressure loss. Counterflow devices enable uniform heat distribution across the heat exchanger and offers a better efficiency in heat transfer compared to the parallel flow approaches. For example, Akshay et. al. [16] experimentally investigated tube in tube heat exchanger with parallel and counter flow arrangements with cold water and hot water used as the fluids and demonstrated a 30% increase in heat transfer rate in the counterflow arrangement when compared to the parallel case.

Researchers have investigated various approaches to further increase the performance of counterflow heat exchangers without incurring severe frictional pressure loss of the working fluid. A successful approach is to use a curved passage to induce secondary flows which enhance the heat transfer process relative to a straight pipe. Mukeshkumar et.al [17] has compared parallel and counterflow configurations of a helically coiled heat exchanger and demonstrated increases in heat transfer coefficient of 5-9% within the laminar flow range. Rennie and Raghavan [18] experimentally reported the heat transfer in a single loop, coil-in-coil heat exchanger and showed that the configuration results in secondary flows that increase the Dean number resulting in an increase in the overall heat transfer coefficient. Kumar et al. [19] have investigated hydrodynamics and heat transfer characteristics of tube-in-tube helically coiled heat exchangers. Naphon [20] studied the thermal performance and pressure drop of a helical-coil heat exchanger with and without helical crimped fins. Naphon concluded that outlet cold water temperature increases with increasing hot water mass flow rate and the average heat transfer rate increases as hot and cold-water mass flow rates increase. Liu and Sakr [21] reviewed passive heat transfer enhancements in heat exchangers and observed that the helical shape of liquid flow passages can promote higher heat transfer rates which are due to the stronger swirling flow and long residence time in the tube. Ali [22] showed enhancements in convective heat transfer coefficient due to helically shaped channels, and that increased values of Nusselt number and friction factor were experimentally obtained at high values of diameter and small values of coil pitch ratio. Ali

concluded that the turbulence and fluid mixing caused by the helical shape is responsible for the enhanced heat transfer and higher frictional pressure loss. Andrzejczyk and Muszynski [23] experimentally investigated the passive and active enhancement methods on a straight and U-bend double tube heat exchanger. They show that for Reynolds number less than 3,000 is the most effective approach for enhancing heat transfer is to employ passive techniques such as a helicoidal turbulator. Bhuiya et al. [24] experimentally studied the influences of triple twisted tapes on heat transfer rate and friction factor. The experimental results demonstrated that the Nusselt number and frictional factor increased with greater twist as compared with a straight tube. Bhuiya et al. [25] explored the effects of double counter twisted tapes on heat transfer and fluid friction characteristics in a heat exchanger tube. The experiments were performed with double counter twisted tapes of varying different twist using air as the fluid in a circular tube turbulent flow regime where the Reynolds number was varied from 6,950 to 50,050. The results showed that the heat transfer rate and frictional factor were 60 to 240% and 91 to 286% higher than that of straight tubes. Similar studies and trends were observed by Bas and Ozceyhan [26], Thianpong et al. [27], and Eiamsa-ard et al. [28].

This paper presents the design and analysis of a novel, additively manufactured compact counter flow heat exchanger. The concept employs helically shaped flow channels, which can be manufactured using current DMLS methods and constraints [29], to increase heat transfer effectiveness over current designs while maintaining acceptable levels of working fluid frictional pressure loss. Section 2 reviews the operation of counterflow heat exchangers and develops a mathematical model that can be used to investigate the performance of the device. Results are presented in Section 3 and a parametric study is presented in Section 4. Using water as the working fluids, heat exchanger designs employing helically shaped passages that meet specified heat transfer requirements, while minimizing the pressure loss and device size, are presented and shown to be advantageous as compared with straight channel devices.

II. COUNTERFLOW HEAT EXCHANGER ANALYTICAL MODEL

This section presents the development of analytical models used to predict the performance of a counterflow heat exchanger with helically shaped flow channels. Subsection 2.1 provides an overview of the basic operation of counterflow heat exchangers. Subsection 2.2 develops a model for straight flow channels without and with radial fins, and Subsection 2.3 extends that model to a heat exchanger in which the flow channels are helically shaped. Subsection 2.4 summarizes the most relevant geometric parameters of the device. The analytical models will then be used in Section 3 to compare heat exchanger performance parameters such as overall heat transfer rates, resulting fluid temperatures, pressure loss, volume, and mass.

Counterflow Heat Exchanger Overview

This paper considers a class of cylindrically shaped counterflow heat exchangers in which the working fluids flow through annular passages. An example of such a heat exchanger is shown in Figure 1. The heat exchanger has an overall length, L, outer diameter,D_o, inner diameter, D_i and consists of two concentric annular passages. In Figure 1, cold fluid with inlet temperature,$T_{c,i}$ flows in the outer annular passage, and hot fluid with inlet temperature,$T_{h,i}$ enters the heat exchanger from the opposite side and flows in the inner annular passage.

Support fins are used to hold the device together, help keep the flow aligned in the axial direction, and augment the conduction heat transfer. For the device shown in Figure 1, the annular passage has been divided into 4 channels using 4 fins, and the inner annular passage has been divided into 8 channels using 8 fins. In this paper, the term passage is used to describe the entire annulus in which a fluid flows, and the term channel is used to describe an individual sector of the passage which has been created through the introduction of fins. The outer, mid, and inner wall thickness are t_o,t_m and t_i respectively.

The inner and the outer passage heights are Ch_i and Ch_o respectively. A unique design feature of the heat exchanger shown in Figure 1 is that the central, cylindrical volume of the device is intentionally left open. This allows the heat exchanger to be effectively placed around the shaft of a turbomachine or other components. In the limit of decreasing inner diameter, the heat exchanger shown in Figure 1 reduces to a device with a cylindrical inner flow passage surrounded by an annular flow passage.

The ideal, steady-state thermal performance analysis for counterflow heat exchangers is described in [30]. The analysis assumes that the flow enters the heat exchanger with fully developed momentum and thermal profiles. With adiabatic external walls and properly sized channel geometry, the hot or cold fluids can flow in either the outer or inner channel with similar performance. Energy balance equations are used to find the required overall heat transfer coefficient. Equation (1) and (2) give the energy balance for the hot and cold fluid, respectively.

$$\dot{q} = \dot{m}_h(h_{h,i} - h_{h,o}) \quad (1)$$

$$\dot{q} = \dot{m}_c(h_{c,o} - h_{c,i}) \quad (2)$$

In Equation (1) and (2), $\dot{q}$ is the heat transfer rate from either hot to cold fluid or from cold to hot fluid,$\dot{m}_h$ is the mass flow rate of hot fluid, $h_{h,i}$ is the inlet enthalpy of the hot fluid, $h_{h,o}$ is the outlet enthalpy of the hot fluid,$\dot{m}_c$ is the mass flow rate of cold fluid, $h_{c,i}$ is the inlet enthalpy of the cold fluid, and $h_{c,o}$ is the outlet enthalpy of the cold fluid. With known mass flow rates, inlet temperatures, and the desired exit temperature of one of the fluids, the heat transfer rate and exit temperature of the other fluid can be determined. Equation (3) gives the heat transfer rate between the two fluids.

$$\dot{q} = U_{req}A_s\Delta T_{lm} \quad (3)$$

In Equation (3), A_s is the surface area available for heat transfer, U_{req} is the overall heat transfer coefficient that is required to achieve the desired heat exchange, andΔT_{lm} is the log mean temperature difference of the fluids given by Equation (4).

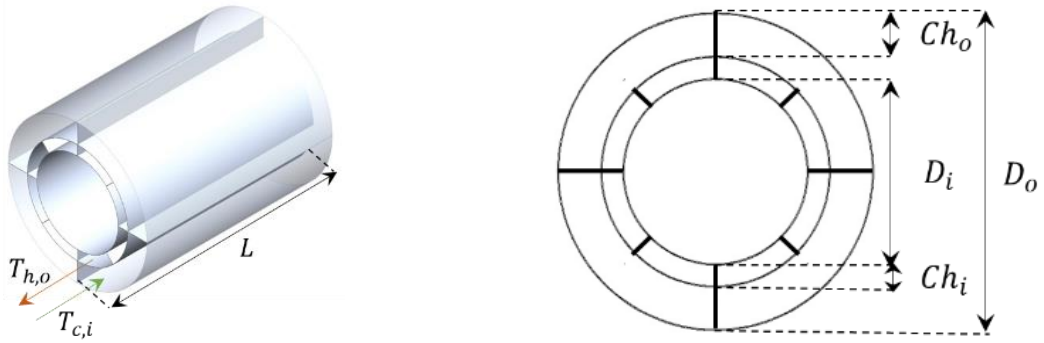

Fig. 1. Annular counter flow heat exchanger with straight channels

$$\Delta T_{lm} = \frac{\Delta T_h - \Delta T_c}{ln(\Delta T_h / \Delta T_c)} \tag{4}$$

In Equation (4), ΔT_h and ΔT_c are the differences of the fluid temperatures at the inlet and outlet of the heat exchanger hot and cold passages, respectively.The achievable overall heat transfer coefficient is the inverse of the total thermal resistance between two fluids. Generally, the coefficient is determined by accounting for conduction and convection resistances between fluids separated by composite plane and cylindrical walls, respectively. In this analysis, no wall thermal resistance is assumed, and the achievable overall heat transfer coefficient is determined from the hot and cold fluid convection coefficients. Equation (5) gives the expression for achievable overall heat transfer coefficient.

$$U_{ach} = \left(\frac{1}{h_h} + \frac{1}{h_c}\right)^{-1} \tag{5}$$

In Equation (5), h_h and h_c are the hot and cold convective coefficients, respectively. The convective heat transfer coefficient is found using equation (6):

$$h = Nu\frac{k}{D_h} \tag{6}$$

In Equation (6), Nu is the Nusselt number, k is the thermal conductivity of the fluid, and D_h is the hydraulic diameter of the flow passage given by Equation (7):

$$D_h = \frac{4A_{crs}}{P} \tag{7}$$

In Equation (7), A_{crs} is the cross-sectional area of the channel and P is the wetted perimeter of the channel. Minimizing the frictional total pressure loss is an important in heat exchanger design. The frictional total pressure loss, ΔP through the channel is given by Equation (8):

$$\Delta P = \frac{fL\dot{m}}{2\rho D_h {A_{crs}}^2} \tag{8}$$

In Equation (8), f is the Darcy frictional factor, L is the channel length, $\dot{m}$ is the mass flow rate of the fluid, $\rho$is the density of the fluid, $D_h$is the hydraulic diameter, and A_{crs} is the cross-sectional area of each channel.

Annular Counter Flow Heat Exchanger with Straight Channels

This subsection develops an analytical model of a counterflow heat exchanger with straight flow channels. Radial fin elements may be added to divide the passages into individual channels. The fins promote greater heat transfer, act as flow straighteners, but also increase flow-surface interaction resulting in larger fluid frictional pressures loss. A schematic of a straight counterflow heat exchanger with 4 channels in the cold section and 8 channels in the hot section was shown in Figure 1.

The flow is assumed to be one-dimensional and follows the shape of the passage. Equation (9) and (10) gives the experimentally determined Nusselt number correlations which are valid for straight channels [31].

$$Nu_D = 4.36 \tag{9}$$

$$Nu_D = \frac{(f/8)(Re_D - 1{,}000)Pr}{1 + 12.7(f/8)^{0.5}(Pr^{2/3} - 1)} \tag{10}$$

$$f = (0.790 ln Re_D - 1.64)^{-2} \tag{11}$$

In the above expressions, f is the Darcy frictional factor,Re_D is the Reynolds number based on hydraulic diameter, and Pr is the Prandtl number. The flow is assumed to be fully developed and is assumed to be under a uniform heat flux. Equation (9) is used when the flow is laminar and $Pr \geq 0.6$. The correlation in Equation (10) is valid for, $3{,}000 \leq Re_D \leq 5\text{x}10^6$,$0.5 \leq Pr \leq 2{,}000$, and $L \geq 10D_h$. Based on the flow regime and Prandtl number, an appropriate *Nu* correlation is chosen, the convective heat transfer coefficient is found for both the hot and cold fluids, and the achievable overall heat transfer coefficient is found using Equation (5).

One approach to improve heat transfer is to divide the channel into passages using fins, which increases the heat exchange area. The achievable overall heat transfer coefficient is given by Equation (12) for the case with fins and the overall fin efficiency is given by Equation (13).

$$U_{ach} = \left(\frac{1}{(\eta_0 h)_h} + \frac{1}{(\eta_0 h)_c}\right)^{-1} \tag{12}$$

$$\eta_0 = 1 - \frac{A_f}{A}(1 - \eta_f) \tag{13}$$

In the above equations, η_0 is the overall fin efficiency,η_f is the efficiency of a single fin, A_f is the fin surface area, and A is the total surface area of the channel. The efficiency of a fin with an adiabatic tip is calculated using Equation (14) [31].

$$\eta_f = \frac{\tanh(mL_f)}{mL_f} \tag{14}$$

$$m = \sqrt{\frac{2h}{k_f t_f}} \tag{15}$$

In the above equations, L_f is the fin length in the radial direction, and m is defined as given in Equation (15), t_f is the fin thickness, h is the convective heat transfer coefficient of the fluid, and k_f is the thermal conductivity of the fin material. The friction factor for laminar flow regime is given by Equation (16) and the Colebrook-White equation [32] is used for the turbulent regime which is given by Equation (17).

$$f_s = 64/Re_D \tag{16}$$

$$\frac{1}{\sqrt{f_s}} = -2\log_{10}\left[\frac{\varepsilon/D_h}{3.7} - \frac{2.51}{Re_D\sqrt{f_s}}\right] \tag{17}$$

In the above equations, f_s is the frictional factor for straight pipes, and ε is the surface roughness of the pipe material.

Annular Counter Flow Heat Exchanger with Helically Shaped Channels

This subsection presents a heat exchanger concept similar to that shown in Figure 1, however, the channels are helically shaped rather than straight. A schematic of the annular counterflow heat exchanger concept with 4 helically shaped channels in the outer passage and 8 helically shaped channels in the inner passage is shown in Figure 2. The helical channel geometry may be characterized by the number of turns, *N*, over the length of the heat exchanger, *L*, or the helical angle, Ψ.

The helical angle is the same as that used to characterize screw fasteners or drill bits and can be defined with respect to either the central axis or normal to the axis. In this paper, the helical angle is defined with respect to a plane that is normal to the axis of the heat exchanger, and straight channel heat exchangers have a helical angle of 90 degrees (*N*=0). As the helical angle decreases below 90 degrees, the number of helical turns increases. The length along the centerline of the helical channel,L_{hlx}, and helical angle, Ψ, are given by Equations (18) and (19). In equations 18 and 19, *N* is the number of helical turns, R_{hlx} is the radius of helix i.e., distance from the axis of the heat exchanger to the centerline of the channel, L_{hlx} is the centerline length of the helical channel, and *L* is the overall length of the heat exchanger device. Equation (18) also demonstrates that for a fixed *N* and *L*, the helical angle for a channel varies radially. The models developed in this paper uses the helical angle at the radial midpoint of each channel. The helical shape of the channel encourages the development of a secondary flow which enhances the heat transfer process. The sense of the vorticity vector that develops due to the curved channel geometry is primarily aligned with flow streamwise direction.The

combination of the spanwise vorticity (due to wall boundary layers) and streamwise vorticity (due to the curved channel shape) results in a complex flow field that can be investigated using numerical methods [33].

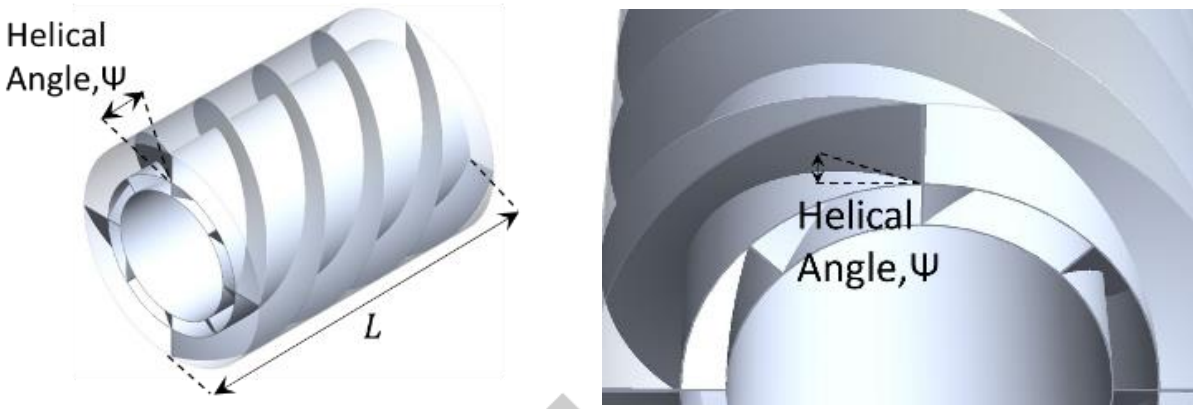

Fig. 2. Annular counter flow heat exchanger with helically shaped passages, *N*=0.5 for the inner passage (*Ψ*=50.7°), and *N*=1 for the outer passage (*Ψ*=49.4°)

$$L_{hlx} = \sqrt{(2\pi N R_{hlx})^2 + L^2} \tag{18}$$

$$\Psi = sin^{-1}(L/L_{hlx}) \tag{19}$$

For the analytical models presented here, the flow is assumed to be one-dimensional and follows the shape of the helical passage. The complex secondary flow effects are captured with augmented heat transfer and friction coefficients that have been experimentally determined for helically shaped channels. The dimensionless Dean number, *De*, is given by Equation (20), and the critical Reynolds number, which is used to identify the transition from laminar to turbulent flow in curved or helical channels, is calculated using Equation (21).

$$De = Re_D(a/R_{hlx})^{1/2} \tag{20}$$

$$Re_{crit} = 2100[1 + 12(R_{hlx}/a)^{-0.5}] \tag{21}$$

In the above equations, a denotes the radius of the channel and, for the heat exchanger design under study in this work, it is equivalent to half of the hydraulic diameter of a single channel. The critical Reynolds number for straight channels is typically taken as 2,100, however the critical Reynolds number for curved channels includes a geometric correction.

For laminar fully developed flow in helical passages with constant heat flux, a Nusselt number correlation has been developed by Manlapaz and Churchill [34] and is given in Equation (22). A Nusselt correlation for turbulent flow developed by Schmidt, valid for $20{,}000 < Re_{crit} < 150{,}000$ and $5 < R_{hlx}/a < 84$ is given by Equation (25). For low Reynolds number $1{,}500 < Re_{crit} < 20{,}000$, Pratt's correlation is recommended and is given by Equation (26). In Equations (25) and (26), Nu_{cv} is the Nusselt number for curved or helical channels and Nu_s (Equation (9) or (10) and is selected based on flow regime) is the Nusselt number for straight channels. In helically shaped channels, the flow generally becomes fully developed within the first half turn. The required convective heat transfer coefficient is given by Equation (3) and the achievable overall heat transfer coefficient is found using Equation (12). A frictional factor correlation for a fully developed laminar flow in a helical passage, proposed by Manlapaz and Churchill [33], is given by Equation (27).

$$Nu_{cv} = \left[\left(4.364 + \frac{4.636}{x_3}\right)^3 + 1.816\left(\frac{\mathrm{De}}{x_4}\right)^{3/2}\right]^{1/3} \tag{22}$$

$$x_3 = \left(1 + \frac{1342}{De^2 Pr}\right)^2 \tag{23}$$

$$x_4 = 1 + \frac{1.15}{Pr} \tag{24}$$

$$Nu_{\mathrm{cv}} = Nu_s\left[1 + 3.6\left(1 - \frac{a}{R_{hlx}}\right)\left(\frac{a}{R_{hlx}}\right)^{0.8}\right] \tag{25}$$

$$Nu_{cv} = Nu_s\left[1 + 3.4\left(\frac{a}{R_{hlx}}\right)\right] \tag{26}$$

$$\frac{f_{cv}}{f_s} = \left[\left(1 - \frac{0.18}{[1 + (35/De)^2)]^{0.5}}\right)^m + \left(1 + \frac{a/R_{hlx}}{3}\right)^2\left(\frac{De}{88.33}\right)\right]^{0.5} \tag{27}$$

$$\mathrm{f_{cv}}\left(\frac{R_{hlx}}{\mathrm{a}}\right)^{0.5} = 0.084\left[\mathrm{Re}\left(\frac{R_{hlx}}{\mathrm{a}}\right)^{-2}\right]^{-0.2} \tag{28}$$

In Equation (27), f_{cv} is the frictional factor for curved passages, f_s is the frictional factor for straight passages, m=2 for $De < 20$, m=1 for $20 < De < 40$, and m=0 for $De > 40$. The appropriate f_s can be calculated based on Re_D and from the correlations given by Equation (16) and (17). Frictional factor for turbulent flow as shown in Equation (28) was developed by Srinivasan [35] and can be used when $\mathrm{Re}\left(\frac{R_{hlx}}{\mathrm{a}}\right)^{-2} < 700$ and $7 < \frac{R_{hlx}}{\mathrm{a}} < 104$.

For all the cases investigated in this work the incident flow is assumed to be aligned to the direction of the channel at the entrance and the exit to the device. In the straight channel case, the incident axial flow is already aligned in the direction of the channel. In the helically shaped channel case, the incoming axial flow to the heat exchanger is now misaligned with the direction of the channel. When that flow enters the helical channel an additional total pressure loss results due to this flow misalignment. This effect can be mitigated by gradually introducing the helical shape after an initial straight passage entry into the heat exchanger. This effect is not considered in this work, and the flow is assumed to enter parallel with the walls of the channel.

Figure 2 showed a heat exchanger with N=0.5 helical turns for the inner passage and one full turn, N=1, for the outer passage. This geometry cannot be fabricated using 3D printing because the fins are cantilevered perpendicular from the wall without support during the printing process. To amend this issue, a fin lean angle is employed, which enables the fins to be self-supported during the print process. A schematic of a heat exchanger with 4 channels in the outer passage and 8 channels in inner passage with fins at a lean angle, θ, is shown in Figure 3. The lean angle is defined with respect to the centerline axis of the heat exchanger. Using this definition, a lean angle of θ=90° corresponds to fins that are perpendicular to the centerline axis and radially outward at any cross-section normal to the axis of the heat exchanger (such as that shown in Figure 1 and Figure 2). For any fixed $\theta<90$ and with any radially varying helical angle, the fins will no longer be perpendicular, but rather are curved in the radial direction when viewed through a cross-section that is normal to the axis of the heat exchanger. Figure 3 shows the complex shape of the fins (with inner Ψ=50.7°, outer Ψ=49.4° and θ=45°) when viewed at a cross-section normal to the axis of the device, as well as the shape of the fins when viewed through a cross-section that cuts parallel through the centerline axis of the device. The cross-sectional area of the channel perpendicular to the flow direction is independent of the lean angle, however the wetted perimeter increases compared to those with θ=90 °(no lean). Thus, the hydraulic diameter changes, which changes the Reynolds number, and changes the achievable overall heat transfer coefficient. The friction factor (Equation 27) and the Nusselt number correlations (Equation 22, 25, and 26) are within their range of validity for all fin lean angles considered in this paper.

In Figure 3, the lean angles of the inner and outer channels would ideally be in opposite directions, aligned favorably with the incoming flow. However, with the heat exchanger 3D printed vertically along the axis, the lean angle must have the same orientation for both the inner and outer passages to support the fins during the fabrication process. Due to this manufacturing constraint, there would be a recirculation region and an additional pressure loss when the flow encounters a lean angle that is opposite to the flow direction. This effect can be mitigated by utilizing a short straight channel entrance and a transition to the full lean angle within the entry portion of the heat exchanger. This effect is not included in the 1-D analytical model presented in this paper, but could be simulated, and the heat exchanger further optimized, using numerical simulations.

Summary of Geometric Parameters

This subsection summarizes the differences in relevant geometric features of a heat exchanger with helically shaped fluid channels as compared with straight fluid channels. These geometric features include the channel length, cross-sectional area, wetted perimeter, and hydraulic diameter. These parameters have a direct impact on the performance, volume, mass, and compactness of the heat exchanger.

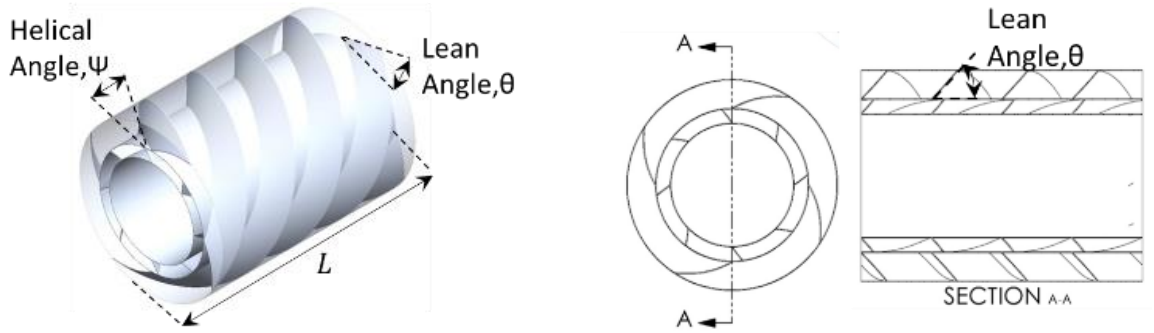

Fig. 1. Annular counter flow heat exchanger with helically shaped passages, N=0.5 for the inner passage (Ψ=50.7°), N=1 for the outer passage (Ψ=49.4°), and θ=45° for both passages

As an example, consider a heat exchanger with D_o=0.28 m,Ch_i=0.005 m, Ch_o=0.005 m, L=0.5 m, and fin and wall thickness of 0.001 m. The heat exchanger has 8 inner (hot) and outer (cold) channels. Table 1 summarizes the important geometric parameters of this heat exchanger as a function of the number of passage helical turns, N, and lean angle, θ. For ease of comparison a baseline case with N=0 and θ =90 ° is used and the helical channel length, L_{hlx}, channel cross sectional area, A_{crs}, perimeter, P, hydraulic diameter, D_h, and compactness for this baseline case are normalized to 1 and all other results presented in Table 1 are relative to this baseline case. As N increases, Ψ decreases (Equation (18) and Equation (19)), L_{hlx} increases, A_{crs}, P decreases, and consequently D_h decreases. When a fin lean angle, θ is introduced, L_{hlx} and A_{crs}do not change compared to the case with no lean, θ=0, however P increases thus decreasing D_h. Therefore, as the number of turns increases the fluid velocity increases (due to decreasing A_{crs}) which in turn makes the flow more turbulent and increases heat transfer at the expense of increased frictional pressure loss. When increasing the length of the heat exchanger two parameters can change. The helical angle changes when heat exchanger length, L, is varied, and the number of turns is kept fixed. For a fixed helical angle, the number of turns changes when the heat exchanger length, L is varied. Figure 4 shows how the helical angle must change when heat exchanger length is varied for a fixed number of helical turns, in this case N=1. In Figure 4, as heat exchanger length increases for a fixed N, the helical angle increases which in turn decrease the cross-sectional area and perimeter as shown in Equation (27) and (28). Figure 4 also shows the change in number of helical turns, N when heat exchanger length is varied for a fixed helical angle (in this case, Ψ =31.4°, calculated for N=1). There is no change in flow cross sectional area and perimeter as the helical angle is fixed, however, the helical length increases as shown by Equation (18).

The compactness of the heat exchanger is defined as the heat transfer surface area to the volume of the heat exchanger. Somewhat arbitrary values of what constituents a compact heat exchanger can be found in the literature, for example for liquid-liquid devices, a value of 400 m^2/m^3 is considered compact, and for gas-gas devices a value of about 700 m^2/m^3 is considered compact [36]. The volume of the heat exchanger shown in Figure 3 does not include the empty cylindrical section and only refers to the actual functional volume of the heat exchanger.

For example, in a heat exchanger with helically shaped channels, increasing the number of turns would does not change the volume of the device, but does increase the heat transfer surface area, thereby increasing the compactness of the device. Table 1 shows that as for a heat exchanger with N=0.5 turns the compactness increases by 5% when compared to the straight heat exchanger design and when the number of turns is increased from 0.5 to 1 the compactness increases by 3%. Introducing lean to the fins increases compactness as well. For example, for N=1 the compactness increases by 2% when the lean angle is decreased from 90°(no lean) to 45°.

III. Modeling Results

This section uses the modeling approach developed in Section 2 to compare heat exchanger performance differences between straight passages and helically shaped passages. In all cases, the heat exchanger is made from stainless steel 316 with density of 8,000 kg/m^3, and has D_o=0.28 m, Ch_i=5 mm, Ch_o=5 mm, and L=0.5 m. The objective is to cool the incoming hot fluid from 368 K to 298 K using the cold fluid which enters the heat exchanger at 278 K. The heat transfer performance and fluid pressure loss for different fluid mass flow rate combinations is compared as a function of the number of turns of the passages and the fin lean angle. The relevant design and performance constraints are summarized in Table 2. For a given mass flow rate, inlet and outlet temperature, Equation (1) is applied for the hot fluid to calculate the heat transfer rate. Using the calculated heat transfer rate, the outlet temperature of the cold fluid is calculated using the same energy balance equation for the cold fluid.

Table 1:Summary of important heat exchanger geometric parameters

Parameter	θ =90°				θ=45°			
	N=0	N=0.5	N=1	N=1.25	N=0	N=0.5	N=1	N=1.25
Ψ	90°	50.7°	31.4°	22.1°	90°	50.7°	31.4°	22.1°
L_{hlx}	1	1.29	1.92	2.66	1	1.29	1.92	2.66
A_{crs}	1	0.77	0.51	0.37	1	0.77	0.51	0.37
P	1	0.78	0.54	0.40	1.02	0.80	0.56	0.42
D_h	1	0.98	0.95	0.91	0.98	0.96	0.92	0.86

Compactness	1	1.05	1.08	1.09	1.02	1.07	1.1	1.12

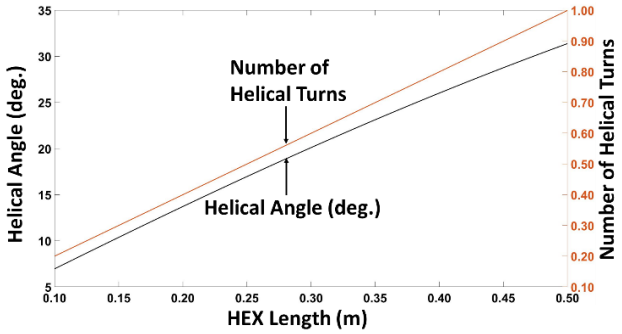

Fig. 4. Heat exchanger length, L vs helical angle, Ψ for fixed helical turns, N=1 (left vertical axis) and heat exchanger length, L vs number of helical turns, N for fixed helical angle, Ψ =31.4° (right vertical axis)

Table 2: Heat exchanger performance parameters with water as working fluid

Parameter Description	Value or Range	Type
Outer diameter, D_o	$\leq 0.28\ m$	Constraint
Overall length, L	$\leq 0.5\ m$	Constraint
U_{ratio}	$= 1$	Constraint
Inlet pressure, P_i	202 kPa	Constraint
Allow frictional pressure loss, ΔP	$\leq$ 5 % of inlet pressure ($\leq$ 10 kPa)	Constraint
Hot fluid inlet temperature, $T_{h,i}$	368 K	Constraint
Hot fluid exit temperature, $T_{h,o}$	298 K	Constraint
Cold fluid inlet temperature, $T_{c,i}$	278 K	Constraint
Wall and fin thickness, t_o,t_i,t_f	1 mm	Constant
Channel heights (inner / outer), $Ch_{i/o}$	-	Variable
Hot fluid mass flow rate, $\dot{m}_h$	0.01 kg/s - 0.1 kg/s	Desired operating range
Cold fluid mass flow rate, $\dot{m}_c$	0.1 kg/s -1 kg/s	Desired operating range
Number of turns, N	-	Variable
Number of fins (inner/outer), $n_{i/o}$	$\leq$ 16	Constraint
Mass of the heat exchanger	$\leq$ 2 kg	Constraint

The log mean temperature difference is then calculated based on the inlet and outlet temperatures of both fluids using Equation (4). Equations (3) and (5) are used to find U_{req} and U_{ach} for different fluid mass flow rate combinations.U_{ratio} is defined as the ratio of U_{ach} to U_{req}, and is equal to 1 when the desired hot fluid exit temperature is achieved.

Performance of an Annular Heat Exchanger with Straight Passages

Table 3 shows the heat exchange, $\dot{q}$, cold fluid exit temperature, $T_{c,o}$,U_{req}, U_{ach}, U_{ratio}, and pressure loss, ΔP,for different mass flow rate combinations in an annular heat exchanger without and with radial fins. The Reynolds number and the Nusselt number are in range with equations and conditions presented in Section 2. In the case of an annular heat exchanger without fins, the U_{ratio} is less than 1 for all mass flow rate combinations, meaning thehot fluid cannot be cooled to the desired temperature using this design. Table 3 also summarizes results when 8 straight fins are added to both the inner and outer passages. A marginal increase in U_{ratio} is achieved compared to the heat exchanger geometry with no fins, however the increase is not significant enough to cool the hot fluid to the desired temperature. The fluid frictional pressure loss with radial fins and without radial fins is summarized in Table 3. Although there is an increase of 4% in U_{ratio} for the heat exchanger design with fins when compared to the design without fins, the pressure loss increases by 11% and 10% in the hot and cold passage respectively when fins are added for $\dot{m}_h$=0.01 kg/s and $\dot{m}_c$=1 kg/s mass flow rate combination. The mass of the heat exchanger also increases from 14.2 to 14.6 kg when fins with 1 mm thickness are added to this design. One approach to achieve a desired U_{ratio} of 1 to increase the length of the heat exchanger. This increase would, however, violate the length design constraint, increase the mass and volume of the heat exchanger, as well as lead to increases in fluid pressure loss. U_{ratio}=1 can also be achieved by increasing the number of fins, but that would mean an increase in mass of the heat exchanger and violating the constraint. Likewise changing diameter, channel heights to achieve U_{ratio}=1 leads to designs violating the performance constraints.

Performance of an Annular Heat Exchanger with Helical Passages

As this work suggests, new additive manufacturing now allow for the introduction of helically shaped fluid passages which can increase the heat transfer performance as compared with straight fluid passages without increasing the overall length of the heat

exchanger or incurring additional mass penalty associated with adding more fins. Table 4 shows how U_{ratio} varies with increasing the number of turns and lean angle.

The U_{ratio} is higher for helical channel heat exchanger when compared to a straight channel heat exchanger (Table 3). As number of turns increases the cross-sectional area of the channel decreaseand the flow velocity and Reynolds number increases.The flow is more turbulent when number of turns are increased, and thus there is better mixing which leads to higher Nusselt number and ultimately better heat transfer and higher U_{ratio}.For a mass flow rate combination of $\dot{m}_h$=0.01 kg/s and $\dot{m}_c$=1 kg/s, when the number of helical turns is increased from N=1 to N=2, theU_{ratio} increases by 36% and the pressure loss increased by 253% and 573% in the hot and cold channels, respectively.The mass of the heat exchanger increases from 14.9 to 15.2 kg when *N* is increased from 1 to 2.

Table 3: Performance of straight annular heat exchanger

$\dot{m}_h$ (kg/s)	$\dot{m}_c$ (kg/s)	$\dot{q}$ (kW)	$T_{c,o}$ (K)	U_{req} (kW/m^2K)	U_{ach} (kW/m^2K)	U_{ratio}		ΔP without fins (kPa)		ΔP with fins (kPa)	
						No fins	fins	Hot	Cold	Hot	Cold
0.1	0.1	30.3	351	3.917	0.150	0.04	0.04	0.002	0.002	0.002	0.003
0.1	1	30.3	286	1.650	0.129	0.08	0.08	0.002	0.048	0.002	0.053
0.01	0.1	3	286	0.165	0.128	0.78	0.81	0.0002	0.005	0.0002	0.005
0.01	1	3	279	0.156	0.133	0.85	0.88	0.0002	0.056	0.0002	0.062

Table 4: U_{ratio} *for annular heat exchanger with helically shaped channels*

$\dot{m}_h$ (kg/s)	$\dot{m}_c$ (kg/s)	U_{ratio}				
		N=0, θ =90°	N=0.5, θ =90°	N=1, θ =90°	N=1, θ =45°	N=2, θ =90°
0.1	0.1	0.04	0.08	0.09	0.09	0.1
0.1	1	0.08	0.20	0.29	0.29	0.37
0.01	0.1	0.81	1.15	1.27	1.30	1.54
0.01	1	0.88	1.40	1.88	1.91	2.56

In some of the mass flow rate combinations, the U_{ratio} exceeds 1, which means that the hot fluid is over-cooled. In such situations, either the geometry can be changed, for example reducing the length of the heat exchanger or decreasing the diameter, to reduce U_{ratio} to 1, or mass flow rate of hot fluid can be increased, or mass flow rate of cold fluid can be decreased. Table 4 also summarizes how the U_{ratio} changes for fins with and without lean. For *N*=1 and for mass flow rate combination of $\dot{m}_h$=0.01 kg/s and $\dot{m}_c$=1 kg/s, theU_{ratio} increases by 2% for the case with lean (θ =45°) when compared to the case without lean(θ =90°). This is due to the increase in heat transfer area surface area that occurs with due to the introduction of the 45° lean angle.

Table 5 summarizes the frictional pressure loss in a heat exchanger with helically shaped fluid passages as a function of the number of turns with and without a wall lean angle for various mass flow rate combinations.Although the lean angle results in a small increase in heat transfer effectiveness, it also increases the pressure loss. For *N*=1 and for mass flow rate combination of $\dot{m}_h$=0.01 kg/s and $\dot{m}_c$=1 kg/s, ΔP increases by 0.2% and 3.3% for hot and cold passages, respectively that have a 45° lean angle as compared to the case without lean (θ =90°).

IV. PARAMETRIC STUDY

In Section 3 the performance of a heat exchanger with a specified diameter, length, and channel heights was compared over a range of fluid mass flow rates for varying number of helical channel turns and fin lean angles. This geometry was based on a current spacecraft application which uses a straight channel counter flow heat exchanger, and it was demonstrated that the heat exchanger could be more compact, thus reducing weight and volume, using helically shaped flow channels. Section 4 now examines how the performance of such a heat exchanger varies with geometric parameters. Heat exchanger length, diameter, number of helical turns, inner channel height, outer channel height, and number of fins are individually varied, and the U_{ratio}, pressure drop, and heat exchanger mass and compactness trends are identified. An initial geometry (D_{max}=0.28 *m*, Ch_i=5 *mm*, Ch_o=5 mm, *L*=0.5 m, and fin and wall thickness = 1 mm) with *N*=0.5 helical turns with no fin lean angle is used as a baseline. A fixed mass flow rate combination of $\dot{m}_h$=0.01 kg/s and$\dot{m}_c$=1 kg/s is used for the comparisons.

Figure 5 and 6 shows performance trends by varying the outer diameter of the heat exchanger from 0.1 m to the allowable D_{max} of 0.28 m. All channel heights are kept fixed at 5 mm. For this comparison, as the outer diameter is increased, the inner diameter also increases, thereby increasing the size of the open, inner section of the heat exchanger. When the outer diameter is reduced to the limiting case of 0.1 m, the heat exchanger no longer has an open, inner section, and the cross-sectional takes the form of an inner circular channel surrounded by an outer annulus. Figure 5 and 6 demonstrates that increasing the outer diameter increases the U_{ratio} and the mass of the heat exchanger but decreases the pressure drop in both the inner and outer passages. At an outer diameter of 0.21 m, a change in the increasing trend of the U_{ratio} and pressure drop (Figure 5) occurs. This is attributable to the larger cross-sectional flow area (leads to decrease in flow velocity and Reynolds number) in which the cold fluid is now laminar, rather than turbulent as was the case for smaller outer diameters. Although the cold flow is laminar for

larger outer diameters, the increasing diameter also increases the area available for heat transfer thereby leading to further increases in the U_{ratio}. For the 0.01 kg/s hot fluid mass flow rate and channel cross-sectional area, the fluid is always laminar even at the smallest outer diameter considered.Heat transfer compactness decreases with increasing diameter as the increasing volume is greater than the increasing heat surface area.

Figure 7 and 8 shows performance trends by varying the overall heat exchanger length from 0.1 m to the allowable $L_{max}$of 0.5 m. As the overall length is increased, relationship between overall heat exchanger length and the length of the helical channels is given by Equation 18. All channels heights are kept at 5 mm, the wall and the fin thickness are 1 mm, and the outer diameter is set to 0.28 m. Figure 7 and 8 shows that U_{ratio} and the mass of the heat exchanger increases, however the pressure drop in both the inner and outer passages decreases as the heat exchanger length is increased from 0.1 to 0.5 m. Increasing the heat exchanger length increases the helical angle, making the passages straighter, see Figure 3. This effect leads to an increase in cross-sectional area and lowers the flow velocity and Reynolds number.Even though the flow becomes laminar for longer lengths the resulting

Table 5: Frictional pressure loss in an annular heat exchanger with helically shaped channels

$\dot{m}_h$ (kg/s)	$\dot{m}_c$ (kg/s)	ΔP (kPa)									
		N=0, θ=90°		N=0.5, θ=90°		N=1, θ=90°		N=1, θ=45°		N=2, θ=90°	
		Hot	Cold	Hot	Cold	Hot	Cold	Hot	Cold	Hot	Cold
0.1	0.1	0.002	0.003	0.005	0.007	0.014	0.018	0.015	0.019	0.065	0.082
0.1	1	0.002	0.053	0.006	0.232	0.016	1.49	0.017	1.543	0.073	10.47
0.01	0.1	0.0002	0.005	0.0004	0.012	0.001	0.031	0.001	0.033	0.004	0.133
0.01	1	0.0002	0.062	0.0004	0.253	0.001	1.46	0.001	1.51	0.004	10.17

increase in heat transfer leads to a continued increase in U_{ratio}.For this geometry and flow rates considered here, this change in the trend with U_{ratio} and pressure drop occurs at an overall length of 0.34 m. For lengths longer that 0.34 m, the cold fluid is turbulent (the hot fluid is always laminar). Heat transfer compactness also decreases with heat exchanger length. The results of Figure 7 can also be used to provide a minimum required heat exchanger length. For example, keeping all other geometric parameters fixed, and with flows rates of $\dot{m}_h$=0.01 kg/s and $\dot{m}_c$=1 kg/s, the heat exchanger must be at least 0.28 m in length to achieve a U_{ratio} of 1. Any extra length to the heat exchanger is not needed unless further cooling of the hot fluid is required.

Figure 9 and 10 shows performance trends by varying the height of the outer channel (cold fluid), and Figure 11 and 12 shows the performance trends by varying the height of the inner channel (hot fluid). Varying the channel height can be accomplished in different ways, such as by adjusting the outer diameter, inner diameter, or wall thickness, and these approaches will lead to different heat exchanger geometries. In this study the outer diameter is fixed, and the variation of channel height is accomplished by varying the inner diameter. The channel heights can be increased until D_i=0 and the inner annular passage becomes a circular passage. The trends varying the outer channel height are shown in Figure 9 and 10. The inner channel height and the outer diameter remain fixed. Increasing the outer channel heights increases the outer channel cross-sectional area and decreases the inner channel cross-sectional area (inner channel radius decreases and thus decreases inner helical angle as shown in Equation 18 and 19). Pressure drop is inversely proportional to cross-sectional area and thus there is a decrease in outer channel pressure drop and increase in the inner channel. An increase in mass (fluid mass increases) and a decrease in heat transfer compactness is seen when the outer channel height is increased.

The trends for varying the inner channel height are shown in Figure 11 and 12. Increasing the inner channel height means the inner diameter decreases and the outer channel height and the outer diameter remains the same. When the inner channel height is increased, the inner cross-sectional area increases resulting in a decrease in pressure drop and Reynolds number. There is no change in outer channel cross-sectional area (outer channel radius is the same and thus no change in outer helical angle) and thus the outer channel pressure drop does not change. With Reynolds number decreasing the heat transfer coefficient decreases and thus U_{ratio} decreases. Similar to the trends shown with variation of the outer channel height, there is a resulting increase in mass and a decrease in heat transfer compactness when the inner channel height is increased. When the inner channel height decreases from 0.1 to 0.05 m the increase in U_{ratio} is 14% and when the height decreases from 0.05 m to 0.005 m the increase in U_{ratio} is 250%. For this geometry, the change inU_{ratio} is minimal when inner channel height decreases from 0.1 m to 0.05 m when compared to that of the decrease from 0.05 m to 0.005 m. Figure 13 and 14 summarizes the effects of increasing the number of fins and thereby increasing the number of fluid passages. Increasing the number of fins increases the heat transfer surface area and thus the U_{ratio}. Increasing the number of fins decreases the fluid cross-sectional area because the fins have a fixed thickness and occupy a greater fraction of the passage cross-sectional area. The increasing number of fins leads to an increase in Reynolds number, meaning that the flow becomes turbulent. This effect contributes to the increase in U_{ratio}. The downside to increase in number of fins is that pressure drop and the heat exchanger mass increases. The heat transfer compactness increases due to the increase in heat transfer surface area with no change in volume.

Figure 15 and 16 shows the effect of varying the number of helical turns, *N*, on device performance. Figure 15 shows U_{ratio} and pressure loss and Figure 16 shows the effect of the number of helical turns on the mass and compactness of the heat exchanger. Increasing helical turns reduces the flow cross-sectional area, which increases the Reynolds number leading to an increase in U_{ratio} as well as an increase the frictional pressure loss. For these cases, the flow is turbulent in both the cold and hot passages. Both the mass and compactness increase due to the increase in heat transfer surface area.

Table 6 shows three different heat exchanger design solutions which meet the goal of U_{ratio}=1 and which satisfy the design constraints presented in Table 2 for a mass flow rate combination of $\dot{m}_h$=0.01 kg/s and $\dot{m}_c$=1 kg/s. Design 1 in Table 6 has the

lowest mass and volume, fits within the geometric design constraints, and meets the goal i.e., U_{ratio}=1. The least frictional pressure loss is achieved with the Design 2, which has a lower frictional fluid pressure loss, 71% lower on hot and 87% lower on cold, as compared with Design 1, and meets the U_{ratio}=1 goal. However, this design has a 72% higher mass and 65% higher volume as compared to Design 1. Design 3 is an example of a compromise between Design 1 and Design 2 in terms of mass, volume, compactness, and pressure drop. Figure 17, 18 and 19 shows the variation in U_{ratio} over a range of flow rates, from 0.01 to 0.1 kg/s for the hot fluid and from 0.1 to 1 kg/s for the cold fluid, for the 3 different designs. In Figure 17, 18, and 19 the sensitivity of U_{ratio} increases as $\dot{m}_h$ approaches 0.01 kg/s and $\dot{m}_c$ approaches 1 kg/s.For Design 1,2 and 3, the U_{ratio} increases by 33%, 20% and 25%, respectively and is due to the flow transitioning from laminar to turbulent in the hot channel. The percentage increase in U_{ratio} due to the flow transition decreases with increase in hot fluid mass flow rate.

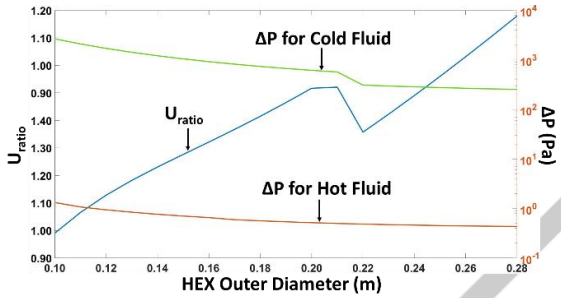

Fig.5. U_{ratio} and pressure drop vs heat exchanger outer diameter

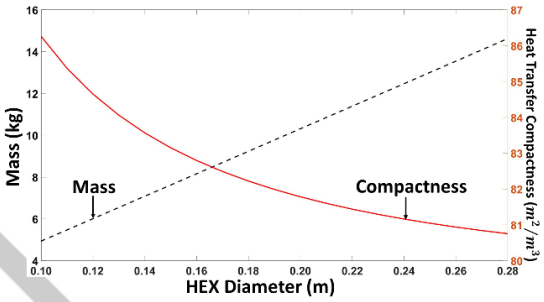

Fig. 6. Mass and HEX compactness vs heat exchanger outer diameter

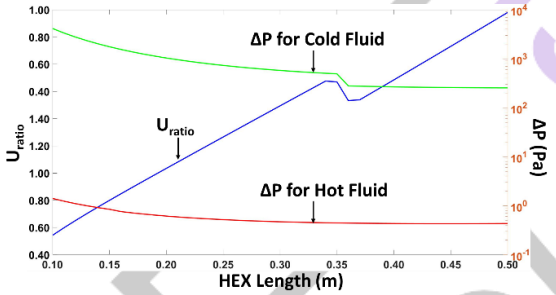

Fig.7. U_{ratio} and pressure drop vs heat exchanger length

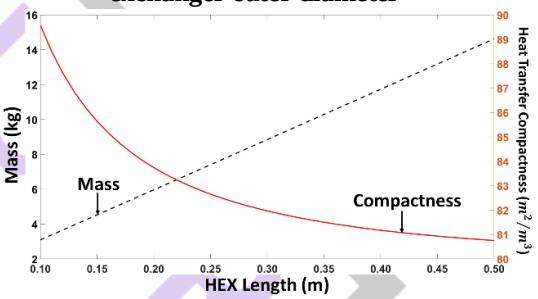

Fig. 8. Mass and HEX compactness vs heat exchanger length

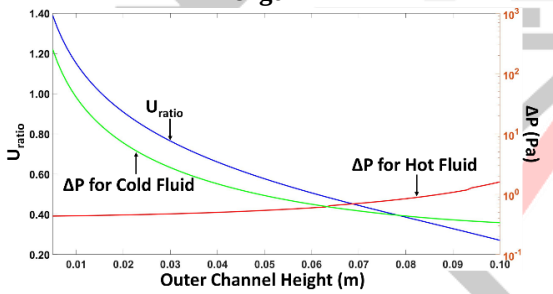

Fig. 9. U_{ratio} and pressure drop vs heat exchanger outer channel height

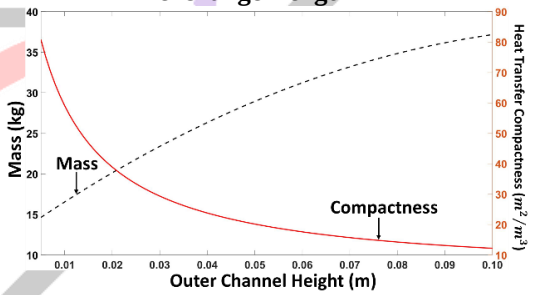

Fig. 10. Mass and heat transfer compactness vs heat exchanger outer channel height

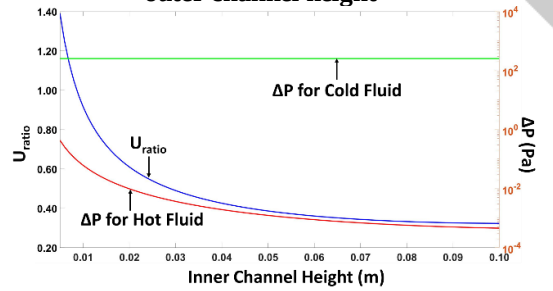

Fig. 11. U_{ratio} and pressure drop vs heat exchanger inner channel height

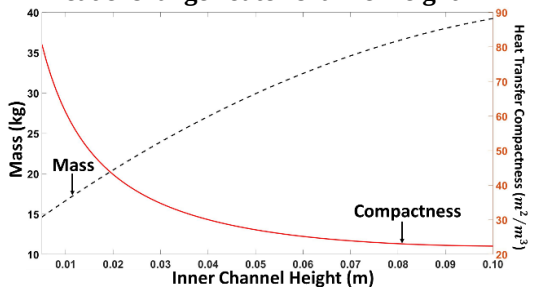

Fig. 12. Mass and heat transfer compactness vs heat exchanger inner channel height

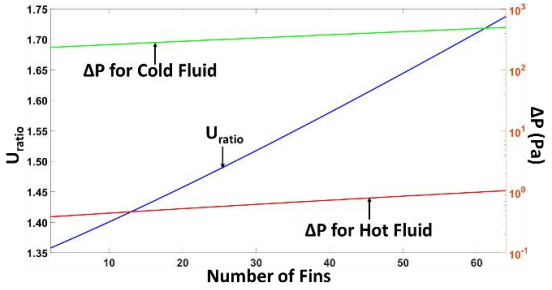

Fig. 13. U_{ratio} and pressure drop vs heat exchanger helical fins

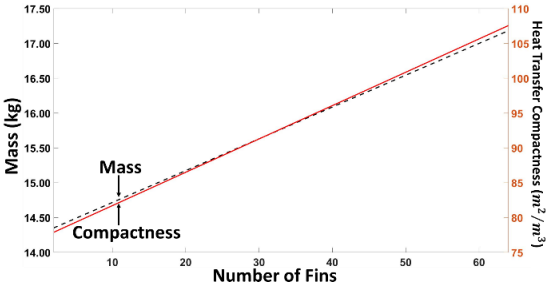

Fig. 14. Mass and heat transfer compactness vs heat exchanger helical fins

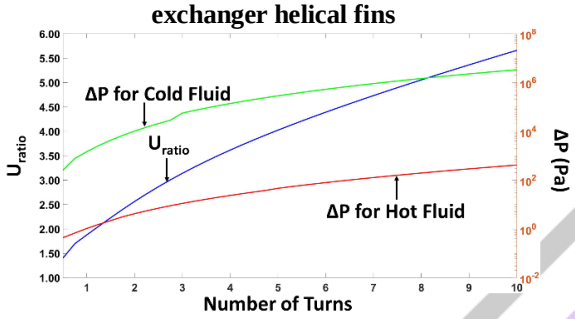

Fig.15. U_{ratio} and pressure drop vs heat exchanger helical turns

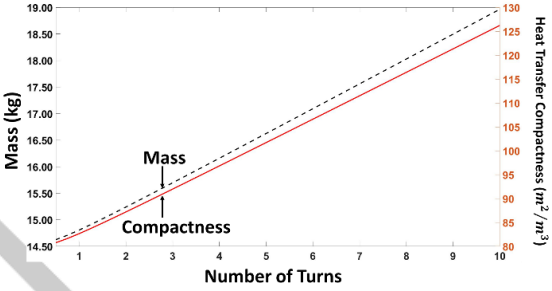

Fig. 16. Mass and heat transfer compactness vs heat exchanger helical turns

Figure 20 shows the variation in pressure drop with mass flow rate in the hot channel for the 3 designs when the cold mass flow rate is fixed at $\dot{m}_c$=1 kg/s. Figure 21 shows the pressure drop variation with mass flow rate in the cold channel when the hot mass flow rate is fixed at $\dot{m}_h$=0.1 kg/s for all the three designs summarized in Table 6.As a final comparison to demonstrate the benefits of helically shaped flow passages, table 7 shows the performance of 3 straight channel heat exchanger designs (1s, 2s, 3s) having the same dimensions of the 3 helical designs in Table 6 but with the straight channels.

Table 6: Heat exchanger design parameters and performance to achieve U_{ratio}=1

Design Number	Length L(m)	Outer Diameter D_o (m)	Channel Height (mm)		Fins		Helical Turns		ΔP (kPa)		Mass (kg)	HEX Volume (cm3)	HEX Compactness (m2/m3)
			Ch_i	Ch_o	n_i	n_o	N_i	N_o	Inner	Outer			
1	0.11	0.11	1	6	3	2	1	1	0.21	9.14	1.10	345.6	102.6
2	0.14	0.14	1	6	8	8	0.5	0.5	0.06	1.19	1.89	571.8	108.5
3	0.12	0.12	1	7	8	5	0.75	1	0.13	6.58	1.44	452.0	104.3

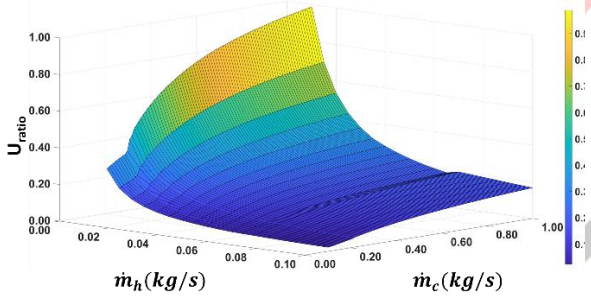

Fig.17. U_{ratio} vs $\dot{m}_h$ vs $\dot{m}_c$ for Design 1

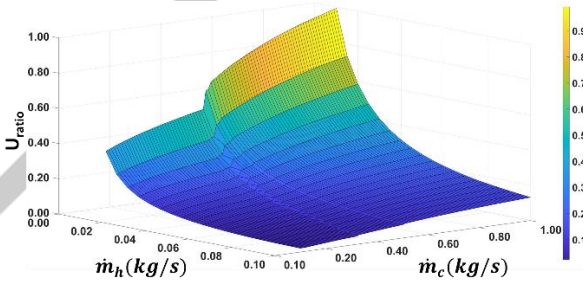

Fig.18. U_{ratio} vs $\dot{m}_h$ vs $\dot{m}_c$ for Design 2

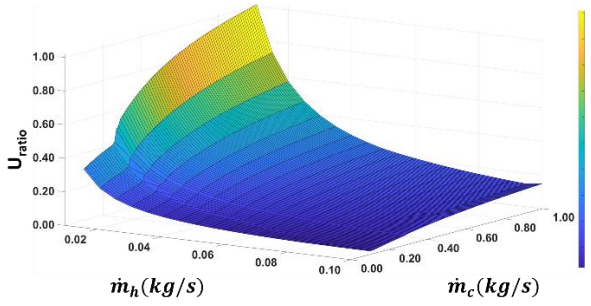

Fig.19. U_{ratio} vs $\dot{m}_h$ vs $\dot{m}_c$ for Design 3

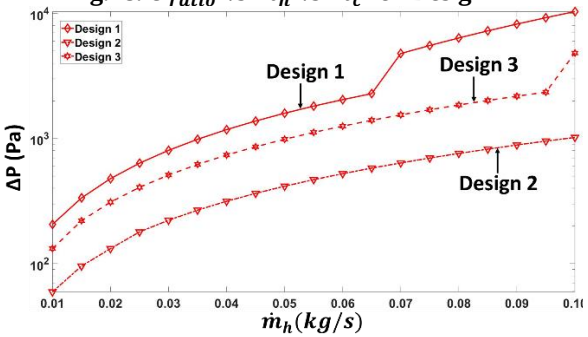

Fig.20. Pressure drop vs $\dot{m}_h$ for Design 1,2 and 3

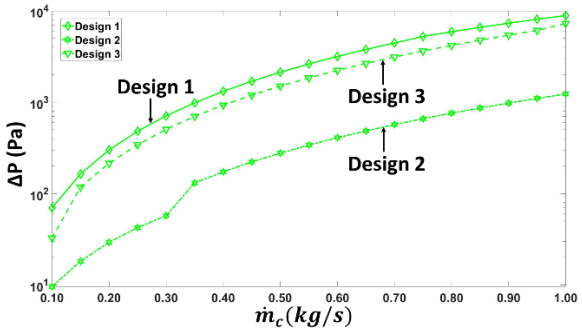

Fig.21. Pressure drop vs $\dot{m}_c$ for Design 1,2 and 3

Even though the pressure drops are within the constraints for all the three designs, the U_{ratio} is less than 1 meaning that the device does not achieve the requisite level of heat exchange. Table 7 also shows the length required to achieve U_{ratio}=1 and the corresponding pressure drop, mass, volume, and heat transfer compactness. The surface area and the volume of the heat exchanger with straight channels is linearly proportional to *L*, and as *L* increases the compactness remains constant. To increase the U_{ratio}=1 in Design 3s, the length must be increased from 0.12 m to 0.29 m, and the mass increases from 1.81 kg to 3.24 kg, which is greater than the design constraint of 2 kg. Decreasing the channel heights would also bring U_{ratio} to 1, however, the frictional pressure loss would then violate the design constraints. For example, decreasing the inner and outer channel height to 0.8 and 0.9 mm in Design 3s would result in U_{ratio}=1, however the frictional pressure loss increases to 0.032 kPa and 14.63 kPa in the hot and cold channels, respectively.

Table 7: Design performance for heat exchanger with straight channels

Design Number	U_{ratio}	ΔP (kPa)		Mass (kg)	Volume Space (cm3)	HEX Compactness (m2/m3)	Length required for U_{ratio} = 1	ΔP (kPa)		Mass (kg)	HEX Volume (cm3)	HEX Compactness (m2/m3)
		Inner	Outer					Inner	Outer			
1s	0.40	0.017	0.053	1.07	345.6	96.6	0.28	0.044	0.132	2.68	863.9	96.6
2s	0.57	0.018	0.049	1.81	571.8	101.0	0.25	0.031	0.087	3.24	1021	101.0
3s	0.42	0.019	0.034	1.34	452.0	89.9	0.29	0.044	0.082	3.17	1073	89.9

Adjusting the geometric design parameters can bring U_{ratio}=1 for the straight channel device but either the frictional pressure loss or the mass is higher than the design constraint. The designs shown in Table 6, which employ helically shaped flow passages, are able to achieve the goal of U_{ratio}=1 and meet all the constraints without increasing the overall length of the heat exchanger.

V. CONCLUSIONS

This work presented the design and analysis of a novel, additively manufactured counter flow heat exchanger which uses helically shaped flow passages. An analytical model of the heat exchanger was developed, and a parametric study was used to assess the performance of the heat exchanger with design variables and given design constraints. General findings, which apply to heat exchangers of this type are:

- Counterflow heat exchangers which employ helically shaped flow passages offer improved heat transfer compared to straight flow passage geometries with working fluid frictional pressure loss as the tradeoff.
- An increase in number of helical turns decreases the channel cross-sectional area which increases flow velocity and Reynolds number thereby making the flow more turbulent and thus increasing the heat transfer rate and frictional pressure drop.

Candidate heat exchanger concepts which meet specified design and DMLS manufacturing constraints were identified and shown to be more compact than straight flow passage variants. As an example, using a water mass flow rate combination of $\dot{m}_h$=0.01 kg/s and $\dot{m}_c$=1 kg/s, D_{max}=0.28 m, Ch_i=5 mm, Ch_o=5 mm, *L*=0.5 m, and fin and wall thickness all set to 1 mm with 8 fins in the inner and outer channels, it was found that:

- The U_{ratio} for the helical passage design with *N*=0.5turns is 59% higher than the straight passage design. However, the frictional pressure loss increased by 100% and 317% for the helical hot and cold passages, respectively, compared to the straight passage design.
- When the number of helical turns is increased from *N*=1 to *N*=2, the U_{ratio} increases by 36%. The frictional pressure loss increases by 300% and 596% for the hot and the cold passages, respectively. However, when the number of helical turns in increased from *N*=1 to *N*=2, the overall length of the device can be reduced from *L*=0.155 m to *L*= 0.077 m, thereby decreasing the mass and volume of the device by 36% and 50.3% respectively, while maintaining U_{ratio}=1.
- A tradeoff between acceptable frictional pressure loss, device mass, and volume compactness can be used to optimize a heat exchanger for a specific application.

- If low mass and volume of the heat exchanger is prioritized, the resulting design typically will sacrifice working fluid frictional pressure loss. For example, when the mass and volume decrease by 24% and 31%, respectively, the frictional pressure loss in the hot and cold channels increase by 61% and 39%, respectively.
- If maintaining lower levels of working fluid frictional pressure loss is prioritized, then the mass and volume of the heat exchanger will be higher. For example, when the pressure loss decreases by 71% and 87% in the hot and cold passages, respectively, the mass and volume of the heat exchanger increases by 72% and 65%, respectively.

The device concept presented in this paper can be applied for various applications in which compactness and space constraints are prioritized, for example for use in spacecraft applications. The analytical model can be extended for different working fluids and operating conditions.

REFERENCES

[1] The Wide Range of Space Mission Applications, Space Mission Engineering: The new SMAD, http://www.sme-smad.com/, 2020 (accessed 25 December 2020)

[2] Michael Izenson, Darin Knaus and Francisco Valentin, Lightweight, Durable PCM Heat Exchanger for Spacecraft Thermal Control, 47th International Conference on Environmental Systems, July (2017),16-20.

[3] Ungar E, Navarro M, Hansen S and Sheth R, Water Phase Change Heat Exchanger System Level Analysis for Low Lunar Orbit, 46th International Conference on Environmental Systems, Jul (2016), ICES-2016-359.

[4] Hasan M.M, Khan L, Nayagam V, and Balasubramaniam R, Conceptual Design of a Condensing Heat Exchanger for Space Systems using Porous Media, Proceedings SAE International Conference for Environmental Systems, July (2005) p. 2.

[5] James A. Nabity, Georgia R. Mason and Robert J. Copeland, A Freezable Heat Exchanger for Space Suit Radiator Systems, SAE International (2008), 01-2111.

[6] G. D. Mathur, Controlling space humidity with heat-pipe heat exchangers, Collection of Technical Papers. 35th Intersociety Energy Conversion Engineering Conference and Exhibit (IECEC) (Cat. No.00CH37022), July (2000), pp. 835-842 vol.2

[7] Kuan-Lin Lee, Calin Tarau and Nathan Van Velson, 47th International Conference on Environmental Systems, July (2017), ICES-162.

[8] Vinod G. Gokhare, Dr. D. N. Raut and Dr. D. K. Shinde, A Review paper on 3D-Printing Aspects and Various Processes Used in the 3D-Printing, International Journal of Engineering Research & Technology, June (2017), Vol. 6 Issue 06.

[9] Tuan D. Ngo, Alireza Kashani, Gabriele Imbalzano, Kate T.Q. Nguyen, David Hui, Additive manufacturing (3D printing): A review of materials, methods, applications and challenges, Composites Part B: Engineering, Volume 143(2018), Pages 172-196, ISSN 1359-8368.

[10] P. S. Kamble, S. A Khoje and J. A Lele, Recent Developments in 3D Printing Technologies: Review, Second International Conference on Intelligent Computing and Control Systems (ICICCS), June (2018), pp. 468-473.

[11] Taha Hasan Masood Siddique, Iqra Sami, Malik Zohaib Nisar, Mashal Naeem, Abid Karim and Muhammad Usman, Low-Cost 3D Printing for Rapid Prototyping and its Application, IEEE, November (2019), 1911.10758

[12] F. Ribeiro, 3D printing with metals, Computing & Control Engineering Journal, Feb (1998), vol. 9, no. 1, pp. 31-38

[13] David Waller, Adam J. Polizzi, Jeremy J. Iten. Feasibility Study of Additively Manufactured Al-6061 RAM2 Parts for Aerospace Applications. AIAA SciTech Forum (2019).

[14] David Waller, David French, Emmanuel Valentin-Hernandez, Demonstration and Characterization of Novel Additive Manufacturing Approaches for Aerospace RF Applications. AIAA SciTech Forum (2018)

[15] Kevin Weed, David Waller, Briana Brown Ph.D., Cristopher Leone, and Matthew Musselman. Additive Manufacturing Applications in Heat Exchangers, Radiators and Heaters, AIAA SciTech Forum (2020)

[16] AkshaykumarMagadum, Aniket Pawar, Rushikesh Patil, Rohit Phadtare. Mr. T. C. Mestri. Experimental Investigation of Parallel and Counter flow Heat Exchanger. International Journal of Advanced Research in Science, Engineering and Technology, March 2016, Vol. 3, Issue 3.

[17] P.C. Mukeshkumar, J. Kuma, S. Suresh, K. Praveen babu. Experimental study on parallel and counter flow configuration of a shell and helically coiled tube heat exchanger using Al2O3 / water nanofluid, J. Mater. Environ. Sci., Volume-3(2012), Issue-4, pp.-766-775.

[18] Timothy J. Rennie and Vijaya G.S. Raghavan, Experimental studies of a double-pipe helical heat exchanger, Experimental Thermal and fluid Sciences, Vol 29(2005),919-924.

[19] V. Kumar, S. Saini, M. Sharma, K.D.P. Nigam, Pressure drop and heat transfer study in tube-in-tube helical heat exchanger, Chemical Engineering Science, Vol 61(2006), 4403–4416.

[20] P. Naphon, Thermal performance and pressure drop of the helical-coil heat exchangers with and without crimped fins, International Communications in Heat and Mass Transfer, Vol 34 (2007) 321–330.

[21] S.Liu and M.Sakr, A comprehensive review on passive heat transfer enhancements in pipe exchangers, Renewable and Sustainable Energy Reviews, Vol. 19(2013),64-81.

[22] Ali, M.E. Free convection heat transfer from the outer surface of vertically oriented helical coils in glycerol-water solution, Heat and Mass Transfer, Vol 40(2004), 615–620.

[23] RafałAndrzejczyk and Tomasz Muszyński Thermal and economic investigation of straight and U-bend double tube heat exchanger with coiled wire turbulator, Archives of Thermodynamics, Vol 40(2019),17-33

[24] M.M.K. Bhuiya, M.S.U. Chowdhury, M. Shahabuddin, M. Saha, L.A. Memone, Thermal characteristics in a heat exchanger tube fitted with triple twisted tape inserts, International Communications in Heat and Mass Transfer, Vol. 48 (2013),124–132

[25] M.M.K. Bhuiya, A.S.M. Sayem, M. Islam, M.S.U. Chowdhury, M. Shahabuddin,Performance assessment in a heat exchanger tube fitted with double counter twisted tape inserts International Communications in Heat and Mass Transfer, Vol. 50 (2014) 25–33
[26] Halit Bas, VeyselOzceyhan, Heat transfer enhancement in a tube with twisted tape inserts placed separately from the tube wall, Experimental Thermal and Fluid Science, Vol. 41 (2012) 51–58.
[27] C. Thianpong, S. Eiamsa-ard, P. Eiamsa-ard, Turbulent heat transfer enhancement by counter/co-swirling flow in a tube fitted with twin twisted tapes, Experimental Thermal and Fluid Science, Vol. 34 (2010), 53–62.
[28] S. Eiamsa-ard, K. Wongcharee, S. Sripattanapipat,3-D Numerical simulation of swirling flow and convective heat transfer in a circular tube induced by means of loose-fit twisted tapes, International Communications in Heat and Mass Transfer, Vol. 36 (2009), 947–955.
[29] Thomas Duda and L. Venkat Raghavan,3D Metal Printing Technology , IFAC-Papers OnLine, Vol 49-29(2016),103-110.
[30] Vindhya Vasiny Prasad Dubey, Raj Rajat Verma, Piyush Shanker Verma & A. K. Srivastava, Steady State Thermal Analysis of Shell and Tube Type Heat Exchanger to Demonstrate the Heat Transfer Capabilities of Various Thermal Materials using Ansys, Global Journals Inc,14-4(2014),25-30.
[31] Frank P Incropera and David P DeWitt, Fundamentals of Heat and Mass Transfer. 4th ed. 1996, John Wiley & Sons, Inc.
[32] Colebrook, C. F.; White, C. M.,Experiments with Fluid Friction in Roughened Pipes, Proceedings of the Royal Society of London. Series A, Mathematical and Physical Sciences,Vol 161-906(1937),367–381.
[33] E. M. Greitzer, Tan C.S and Graf M.B,2007, Internal Flow Concepts and Applications, Cambridge University Press.
[34] Romeo l. Manlapaz & Stuart W. Churchill, Fully developed laminar convection from a helical coil, Chemical Engineering Communications, Vol 9:1-6 (1981), 185-200.
[35] Srinivasan, P. S., Nandapurkar, S. S. and Holland, F. A, Pressure drop and heat transfer in coils, Chemical. Engineering, Vol 218 (1968),113-119.
[36] Qi Li,GillesFlamant, Xigang Yuan, Pierre Neveu, Lingai Luo, Compact heat exchangers: A review and future applications for a new generation of high temperature solar receivers, Renewable and Sustainable Energy Reviews ,Vol 15 (2011),4855-4875.